universe

Review

Ultra-High-Energy Astroparticles as Probes for Lorentz Invariance Violation

Rodrigo Guedes Lang [1,*], Humberto Martínez-Huerta [2] and Vitor de Souza [3]

[1] Erlangen Centre for Astroparticle Physics, Friedrich-Alexander-Universität Erlangen-Nürnberg, Erwin-Rommel-Str. 1, D-91058 Erlangen, Germany
[2] Departmento de Física y Matemáticas, Universidad de Monterrey, Avenida Morones Prieto 4500, San Pedro Garza García 66238, NL, Mexico
[3] Instituto de Física de São Carlos, Universidade de São Paulo, São Carlos 13566-590, SP, Brazil
* Correspondence: rodrigo.lang@fau.de

Abstract: Compelling evidence for Lorentz invariance violation (LIV) would demand a complete revision of modern physics. Therefore, searching for a signal or extending the validity of the invariance is fundamental for building our understanding of the extreme phenomena in the Universe. In this paper, we review the potential of ultra-high-energy astroparticles in setting limits on LIV. The standard framework of LIV studies in astroparticle physics is reviewed and its use on the electromagnetic and hadronic sectors are discussed. In particular, the current status of LIV tests using experimental data on ultra-high-energy photons and cosmic rays is addressed. A detailed discussion with improved argumentation about the LIV kinematics of the relevant interactions is shown. The main previous results are presented together with new calculations based on recently published astrophysical models.

Keywords: Lorentz invariance violation; UHECR; UHE photons

check for updates

Citation: Lang, R.G.; Martínez-Huerta, H.; de Souza, V. Ultra-High-Energy Astroparticles as Probes for Lorentz Invariance Violation. *Universe* **2022**, *8*, 435. https://doi.org/10.3390/universe8080435

Academic Editor: Maciej Rybczynski

Received: 9 June 2022
Accepted: 18 August 2022
Published: 22 August 2022

1. Introduction

Lorentz invariance is one of the fundamental symmetries in the standard model (SM) of elementary particles. There is renewed interest in the community in testing the limits of its validity given that grand unified theories, such as quantum gravity and string theory, speculate about a certain degree of Lorentz invariance violation (LIV) [1–10].

Most such LIV effects are expected to be small. However, the incredibly high energies of ultra-high-energy (UHE, $E > 10^{18}$ eV) astroparticles, the extreme distances they travel to Earth, and the current level of experimental precision and of the high exposure of observatories in operation makes them promising probes for LIV.

Cosmic and gamma-ray observations have been used to set strong constraints to LIV [11]. Examples of the most explored channels are: (a) changes in the kinematics of processes such as photo-pair production [12–19], (b) processes forbidden in the SM, such as photon splitting and decay [20,21], and Cherenkov radiation in vacuum [22–24], and (c) energy-dependent time delay in photons [25,26].

In this review, we summarize these efforts, discussing the current state-of-the-art analyses and their limitations. First, in Section 2, we present the most common phenomenological framework used in astrophysical tests of LIV. Next, in Sections 3 and 4, we discuss the most up-to-date results and limits obtained with UHE photons and cosmic rays, respectively. The dependence of these analyses on astrophysical models is also explored. Finally, in Section 5, we address our final remarks and prospects for future LIV studies using UHE astroparticles.

2. LIV Framework

The astrophysical corrections of LIV can be addressed via a family of modified dispersion relations (MDR) for each type of particle (see, for instance, [1] and Refs. therein),

$$E_a^2 = m_a^2 + p_a^2 \left(1 + \sum_{n=0,1,2,...} \delta_{a,n} \, E_a^n\right), \tag{1}$$

where E_a and p_a are the energy and momenta, and δ is the LIV parameter for the a-particle.

In the special case of photons ($m_\gamma = 0$), the MDR is,

$$E_\gamma^2 = p_\gamma^2 \left(1 + \sum_{n=0,1,2,...} \delta_{\gamma,n} \, E_a^n\right), \tag{2}$$

where E_γ and p_γ is the energy and momenta and $\delta_{n,\gamma}$ stands for the photon LIV parameter. The positive sign corresponds to the so-called superluminal phenomena and the minus to the subluminal. Using one leading order n at a time, when $n = 0$, the LIV correction corresponds the so-called maximal velocity of photons. If $n = 1$ or $n = 2$, the LIV scale of the correction can be expressed by $E_{\rm LIV}^{(n)} = (|1/\delta_{a,n}^n|)$.

Astrophysical tests had settled strong constraints on the different LIV parameters [1]. For instance, for the subluminal side, the LIV modified pair production interaction on EBL ($\gamma\gamma_{EBL} \to e^+e^-$) bounded $\delta_{\gamma,1} \geq -8.3 \times 10^{-30}$ eV^{-1} $\left(E_{\rm LIV}^{(1)} \geq 1.2 \times 10^{29} \text{ eV}\right)$ and $\delta_{\gamma,2} \geq -1.74 \times 10^{-43}$ eV^{-2} $\left(E_{\rm LIV}^{(2)} \geq -2.4 \times 10^{21} \text{ eV}\right)$, using TeV gamma rays [13], and ref. [27] constrained $\delta_{\gamma,2} > 3.46 \times 10^{-45}$ eV^{-2} $\left(E_{\rm LIV}^{(2)} \geq 1.7 \times 10^{22} \text{ eV}\right)$ through LIV air shower suppression. On the other hand, astrophysical superluminal tests usually derive stronger limits, see, for instance, [28], which by the absence of LIV photon decay ($\gamma \to e^+e^-$) effects on gamma rays reports $\delta_{\gamma,0} \leq 7.1 \times 10^{-19}$, as well as $\delta_{\gamma,1} \leq 3.46 \times 10^{-67}$ eV^{-1} $\left(E_{\rm LIV}^{(1)} \geq 1.7 \times 10^{33} \text{ eV}\right)$, and $\delta_{\gamma,2} \leq 1.6 \times 10^{-51}$ eV^{-2} $\left(E_{\rm LIV}^{(2)} \geq 2.5 \times 10^{25} \text{ eV}\right)$ by the lack of photon splitting ($\gamma \to 3\gamma$). Furthermore, for a collection of Lorentz violating limits in the context of the standard model extension [5] including other SM sectors and dimensions, see the tables in [29].

3. Testing LIV with UHE Photons

No UHE photon has been detected so far [30–32]. The identification of a UHE photon source would lead to very precise and strong limits on LIV. UHE cosmic rays (UHECR) interact with the photon background producing pions. The neutral ones rapidly decay, producing UHE photons which could, in principle, be detected on Earth [33,34] as a secondary flux of UHE photons.

As first proposed in [17,35] and further developed by in [14], if subluminal LIV ($\delta_{\gamma,n} < 0$) is considered, the interaction rate of UHECRs with background photons decreases, leading to an increase in the expected number of UHE photons arriving on Earth.

3.1. Propagation of UHE Photons Considering LIV

Photons may be absorbed on their way to Earth, producing an electron–positron pair when interacting with the photon background ($\gamma\gamma_{\rm bg} \to e^-e^+$) [36]. The mean free path of the interaction is determined by the energy distribution of the background photons and the kinematics of the pair production. In an LI scenario, the mean free path is such that most extragalactic UHE photons are expected to be absorbed. If LIV in the electromagnetic sector is considered, on the other hand, the kinematics of the interaction is expected to be modified [11]. The energy threshold for the pair production considering LIV effects is given by [12,14–17,20]

$$\epsilon_{\rm th}(E_\gamma) = \frac{m_e^2}{E_\gamma} - \frac{\delta_{n,\gamma} E_\gamma^{n+1}}{4}, \tag{3}$$

where E_γ and ϵ are, respectively, the energies of the UHE and background photons, m_e is the electron mass, and $\delta_{n,\gamma}$ is the LIV coefficient. The LIV energy threshold (ϵth) can be larger or smaller than the Lorentz-invariant (LI) case, depending on the sign of $\delta_{n,\gamma}$ in the last term of the equation.

Figure 1 shows the threshold energy for the background photon as a function of the energy of the UHE photon for different subluminal LIV coefficients of order $n = 0$. Similar results are found for higher orders. In a LI scenario, the dominant fields are the extragalactic background light (EBL) for $E \lesssim 10^{14}$ eV, the cosmic microwave background (CMB) for $10^{14} \lesssim E/\text{eV} \lesssim 10^{17}$, and the radio background for $E \gtrsim 10^{17}$ eV. When subluminal (superluminal) LIV is considered, the threshold increases (decreases) with respect to the LI scenario and, thus, fewer (more) interactions are expected. The energy above which this effect becomes significant decreases with increasing absolute values of the LIV coefficient. The survival probability, P_{surv}, of a photon emitted at redshift z, with energy E_γ is obtained by the following expression,

$$P_{\text{surv}} = \exp\left(- \int_0^z \mathrm{d}z \frac{c}{H_0(1+z)h(z)} \int_{-1}^{1} \mathrm{d}\cos\theta \frac{1-\cos\theta}{2} \int_{\epsilon_{\text{th}}}^{\infty} \mathrm{d}\epsilon \; n(\epsilon, z)\sigma(E_\gamma, \epsilon, z) \right), \quad (4)$$

where H_0 and $h(z)$ are the cosmological terms, $\sigma(E_\gamma, \epsilon, z)$ is the Breit–Wheeler cross-section [37], and $n(\epsilon, z)$ is the distribution of background photons.

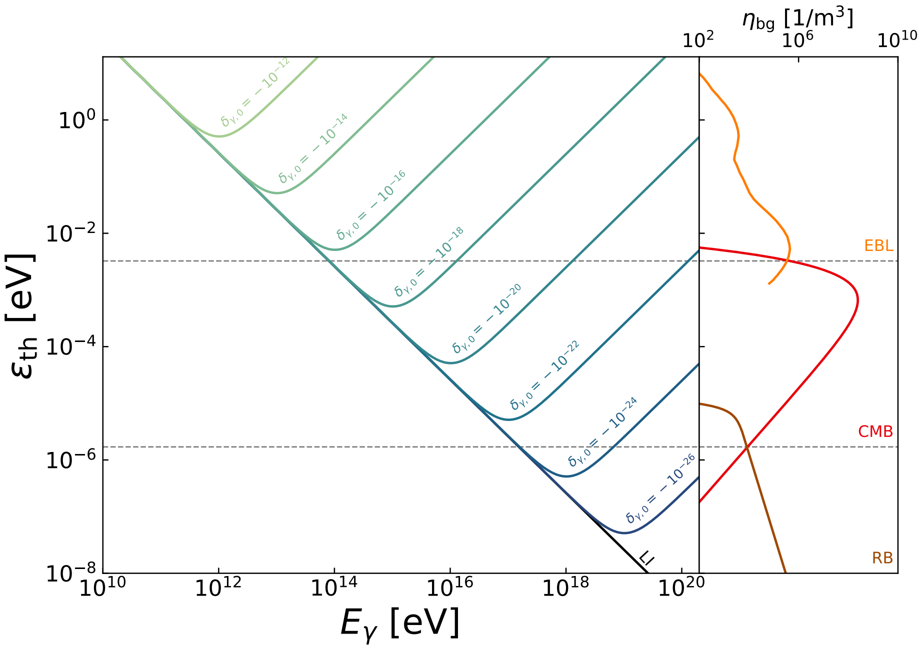

Figure 1. Energy threshold for the pair production as a function of the energy of the propagating photon. The black line shows the results for a LI assumption, while the different colored lines show the results for different subluminal LIV coefficients. The right panel shows the background distribution for that given energy. The dashed lines indicate the region in which each background is dominant. For the EBL, the model in [38] was used as an example. For the RB, the parameterization from [39] was used.

Figure 2 shows the survival probability as a function of the energy for UHE photons emitted at $z = 0.001$, $z = 0.01$ and $z = 0.1$ under different subluminal LIV assumptions. For large LIV coefficients and high energies, the survival probability is increased up to the point where no photons are absorbed. The limiting assumptions, LI ($\delta = 0$) and the maximum LIV ($\delta \to -\infty$), in which no interaction happens at all energies, are shown by the black and red lines, respectively.

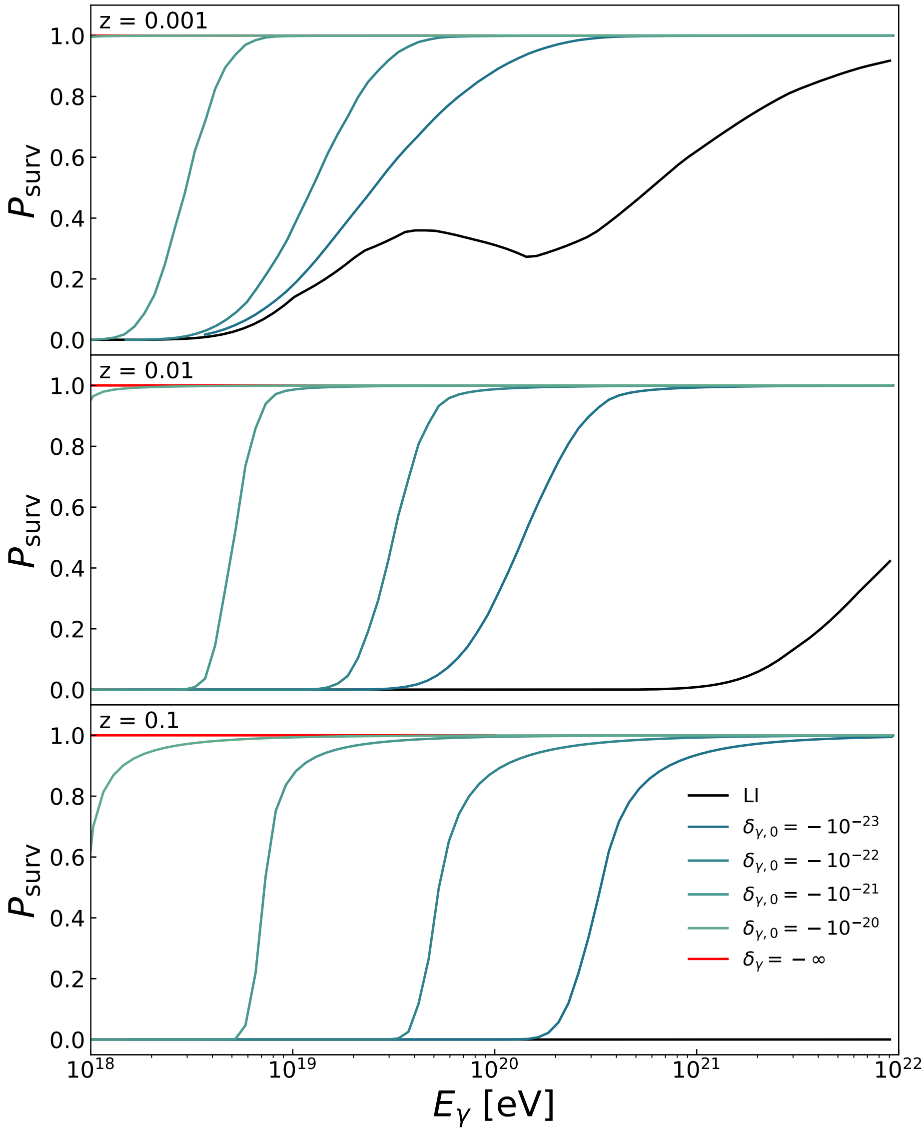

Figure 2. Survival probability as a function of the propagating photon energy. The black line and red line show the limiting cases, i.e., LI and maximum LIV, while the different colored lines show the results for different subluminal LIV coefficients. The three panels correspond to different values of redshift.

3.2. Searching for LIV in UHE Photon Data

When superluminal LIV in considered in photon propagation, the survival probability of the UHE photon is reduced. Since no UHE photon event has yet been detected, it is not straightforward to use current UHE data to search for a decrease in the expected flux.

When subluminal LIV is considered, the survival probability of the UHE photon increases allowing the calculation of upper limits on the LIV coefficients based on the measured upper limits of UHE photons. Several works have used this technique [14,17,35,40]. Since no UHE photon source was detected, only secondary photons produced in the propagation of UHECR are considered in the calculation. As such, the flux of UHE photons arriving on Earth is highly dependent on the UHECR astrophysical model: spacial distribution of the sources, emission energy spectra and chemical composition [41]. Thereby, as first discussed in [14], LIV limits imposed by this technique are highly dependent on the astrophysical assumptions about the UHECR sources.

In phenomenological studies [42], homogeneously distributed sources of UHECRs are usually considered to emit cosmic rays isotropically with energy spectra described by

$$J^A_{\mathrm{UHECR}}(E) = f_A E^{-\Gamma} e^{-\frac{E}{ZR_{\max}}}, \tag{5}$$

where A and Z denote, respectively, the atomic mass and charge for each species of emitted nuclei. The fraction of a given species, f_A, the spectral index, Γ, and the maximum rigidity attainable by the sources, $R_{\max}$, are free parameters and vary between different astrophysical models. Chemical composition is usually divided into five major groups almost equally separated in $\ln A$, with five representative nuclei, ^{1}H, ^{4}He, ^{14}N, ^{28}Si and ^{56}Fe. Such a simplistic description is justified by the lack of knowledge about the sources of UHECR.

Following the procedure proposed in [14], we calculated LIV limits for several astrophysical models covering the phase space of Equation (5) to illustrate their influence on the LIV limits. UHECR propagation is simulated with the state-of-the-art Monte Carlo package `CRPropa 3` [43]. The propagation of the secondary UHE photons is then performed using the package `EleCa` [44], with an implementation of the LIV corrections described in Section 3.1. The simulated energy spectrum of UHECR is normalized to the energy spectrum measured by the Pierre Auger Observatory [45] at $E = 10^{18.75}$ eV. Finally, the LIV limit is obtained as the smallest absolute value of the LIV coefficient for which the predicted flux is more intense than the upper limits imposed by the Pierre Auger Observatory [30–32].

Figure 3 shows the logarithmic order of the LIV limit imposed for each combination of maximum attainable rigidity at the sources and spectral index for the two extreme compositions at the sources, pure proton and pure iron. The results cover all the possibilities, ranging from not being sensitive to LIV up to the case where the model would be inconsistent with data even under a LI assumption. The largest dependence comes from $R_{\max}$. For small maximum rigidities, no cosmic ray will be accelerated up to enough energies to produce UHE photons and, thus, modifying the propagation of UHE photons will have no effect. For large maximum rigidities, on the other hand, too many photons are produced, surpassing the upper limits on the UHE photon flux measured by the Pierre Auger Observatory even without increasing the threshold of the pair production. The composition also plays an important role. For heavy compositions a larger fraction of the phase space of models is allowed under an LI assumption. On the other hand, a larger fraction of the phase space is also not sensitive to LIV.

LIV Limits from Different UHECR Astrophysical Models

UHECR astrophysical models are expected to describe current energy spectrum and composition measurements [45–49], reducing the allowed phase space of Figure 3. In Table 1, we present a collection of phenomenological models for the UHECR sources which can either be described by Equation (5) or be approximated by it.

Table 1. List of UHECR models used. The middle column specifies the model when multiple ones come from the same reference.

Model	Details	Reference
Berezinsky et al. '02	—	[50]
Allard et al. '08 (a)	pure He	[51]
Allard et al. '08 (b)	pure CNO	[51]
Allard et al. '08 (c)	pure Si	[51]
Aloisio et al. '15	—	[52]
Taylor et al. '15 (a)	$n = 0$	[53]
Unger et al. '15 (a)	fiducial model	[54]
Unger et al. '15 (a)	galactic abundance	[54]
Pierre Auger Collaboration '17 (a)	SPG	[42]
Pierre Auger Collaboration '17 (a)	STG	[42]

Table 1. *Cont.*

Model	Details	Reference
Pierre Auger Collaboration '17 (a)	SPD	[42]
Pierre Auger Collaboration '17 (a)	CTG ($\gamma = -1.03$)	[42]
Pierre Auger Collaboration '17 (a)	CTG ($\gamma = +0.87$)	[42]
Pierre Auger Collaboration '17 (a)	CTD	[42]
Pierre Auger Collaboration '17 (a)	CGD	[42]
Muzio et al. '20	—	[55]
Luce et al. '22	—	[56]

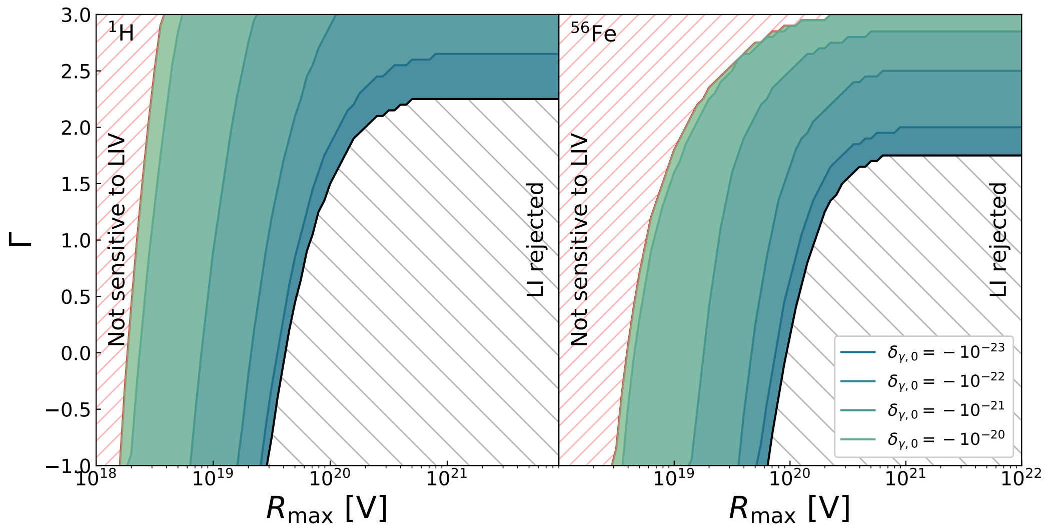

Figure 3. Limits on the subluminal LIV coefficient for the phase space of generic UHECR models. The left and right panels are, respectively, for a pure composition of proton and iron. The shaded red area shows the region of the phase space for which the models are not sensitive to LIV. The shaded black area shows the region already ruled out even in a LI scenario. The different colors show the regions in which the imposed limits would be of a given logarithmic order.

Figures 4–6 show the limits on LIV in photon sector for orders $n = 0, 1, 2$ considering each model from Table 1. The range of limits is quite broad, covering from complete insensitivity to LIV up to $\delta_{\gamma,0} > -10^{-22}$, $\delta_{\gamma,1} > -10^{-42}\ \mathrm{eV}^{-1}$ $\left(E_{\mathrm{LIV}}^{(1)} > 10^{42}\ \mathrm{eV}\right)$ and $\delta_{\gamma,2} > -10^{-60}\ \mathrm{eV}^{-2}$ $\left(E_{\mathrm{LIV}}^{(2)} > 10^{30}\ \mathrm{eV}\right)$, which, for $n = 1$, would be 13 orders of magnitude more restrictive than current subluminal LIV limits obtained in the photon sector using TeV gamma rays [11,13]. This emphasizes once more the strong model dependence of these results. A study comparing the capability of these models to describe UHECR data is outside the scope of this work.

A further reduction of the allowed phase space of UHECR models is expected in the near future with the ongoing upgrade of current facilities, in particular, the Auger-Prime [57,58] at the Pierre Auger Observatory and the TAx4 [59] at the Telescope Array experiment. Future data obtained with the upgraded experiments will improve current statistics, allowing a better description of the spectral features, specially the suppression, which has a direct impact on the possible values for the spectral index and for the maximum power of acceleration of the sources. AugerPrime will also present the capability of investigating the presence of a proton component at the highest energies. If this is confirmed, models which predict a larger flux of UHE photons will be preferred and, consequently, the possibility of imposing restrictive LIV limits is favored. Future experiments such as the Probe of Extreme Multi-Messenger Astrophysics (POEMMA) [60] and Global Cosmic Ray Observatory (GCOS) [61] are expected to shrink the phase space even further in the years to come, softening the model dependence of current LIV studies using UHECR.

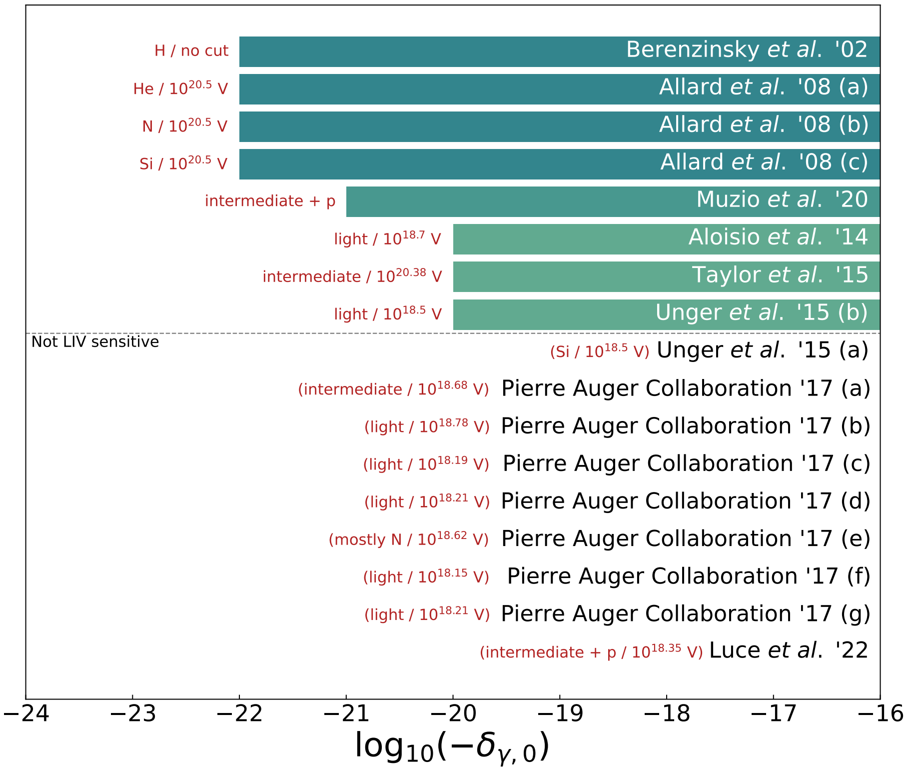

Figure 4. Logarithmic order of the limits on subluminal LIV of order $n = 0$ imposed for each UHECR model. The models below the dashed lines are insensitive to LIV using this technique and, thus, no limits could be imposed. The red texts show a brief description about the two leading features of the models: its composition and maximum attainable rigidity at the sources.

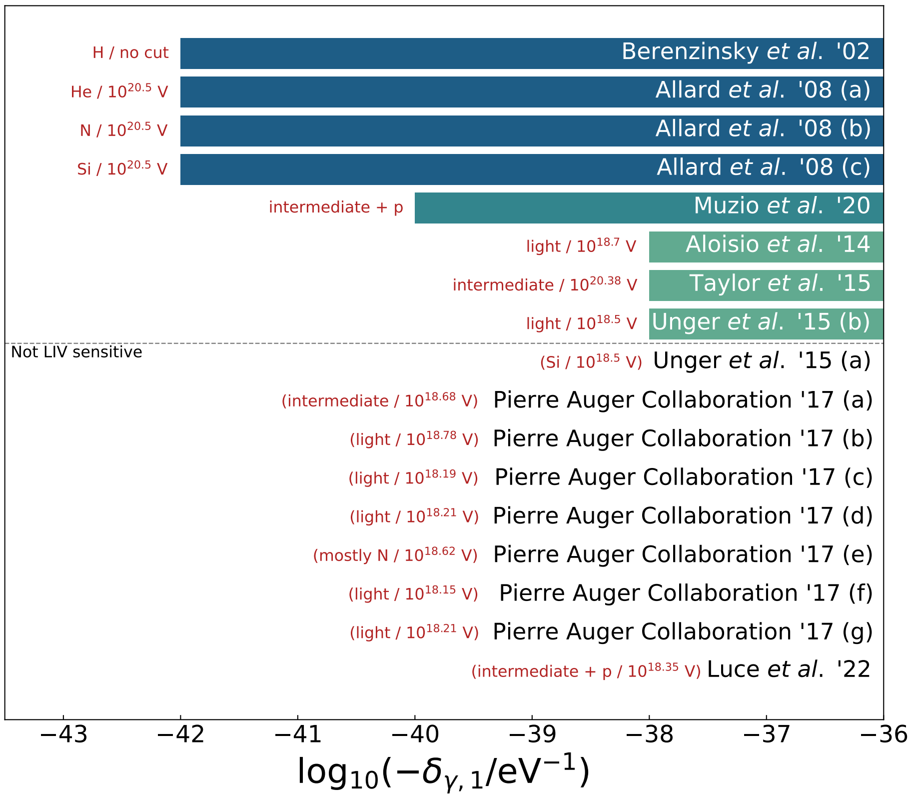

Figure 5. Same as Figure 4, but for $n = 1$.

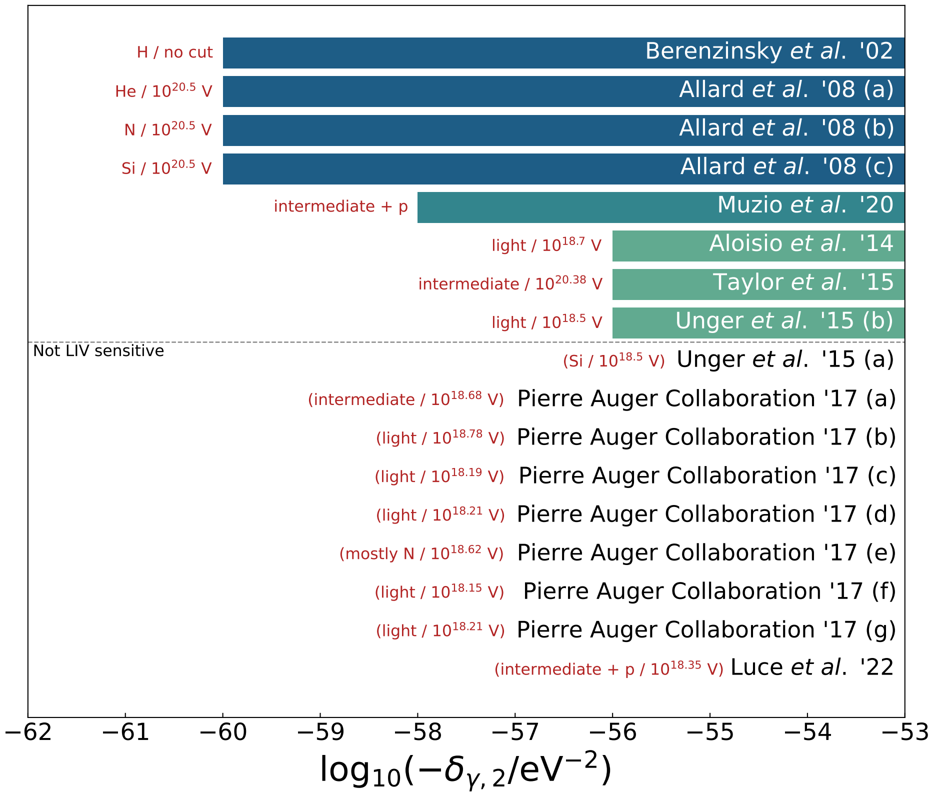

Figure 6. Same as Figure 4, but for $n = 2$.

4. Testing LIV with UHECR

As first proposed independently by Greisen and by Zatsepin & Kuzmin [62,63], the propagation of UHECR at energies of a few tens of EeV is limited by interactions with the photon background. A sharp decrease in the attenuation length of protons is expected above $E \sim 10^{19.5}$ eV due to photopion production ($p + \gamma_{\rm bg} \rightarrow \Delta^+ \rightarrow p/n + \pi^{0/+}$). Furthermore, at these energies, the propagation of heavier nuclei is restricted to a few tens of Mpc by the photodisintegration, through which the nucleus emits a nucleon and becomes a lighter chemical species (${}^{A}N + \gamma_{\rm bg} \rightarrow {}^{A-1}N + p/n$). The emission of two or more nucleons is also possible, but rates are considerably smaller. At lower energies, 10^{18} eV $\lesssim E \lesssim 10^{19.5}$ eV, the propagation is dominated by pair production ($p + \gamma_{\rm bg} \rightarrow p + e^- + e^+$).

These interactions create a propagation horizon, which, combined with the maximum power of acceleration of the sources, leads to suppression at the highest energy end of the spectrum [42] and increases the relative contribution of local sources located up to a few tens of Mpc [64,65]. The relative contribution to the suppression coming from the propagation horizon and from the acceleration limitations is yet to be clarified and differs for each UHECR phenomenological models (see, e.g., Table 1).

If LIV is considered in the hadronic sector, the kinematics of these interactions is modified, leaving imprints that could be detected in UHECR data. Below, we develop further the previous calculations [15,66] of photopion production and photodisintegration under LIV assumption.

4.1. Kinematics of Interactions of UHECR with the Photon Background Considering LIV

The kinematics of any interaction in the form of $(a + b \rightarrow c + d)$ can be solved by imposing energy-momentum conservation such as

$$s^{\rm init} = (E_a + E_b)^2 - (\vec{p}_a + \vec{p}_b)^2 = s^{\rm final} = (E_c + E_d)^2 - (\vec{p}_c + \vec{p}_d)^2, \tag{6}$$

where s is the square of the total rest energy in the center-of-mass reference frame (CMS). Following the MDR in Equation (1), we also define the square of the energy of the particle i in the reference frame where its momentum is zero as

$$s_i = E_i^2 - p_i^2 = m_i^2 + \delta_{i,n} E_i^{(n+2)}. \tag{7}$$

The last term incorporates the LIV effects and can be seen as a shift in the effective mass of the particle. For the cases treated here, b represents the background photon, with energy ϵ, for which no LIV is considered and, thus, $m_b = 0$ and $\delta_b = 0$. The energies of the outgoing particles, E_c and E_d, are unknown and can be expressed as a function of the inelasticity, K, of the interaction,

$$\begin{aligned} E_c &= K E_a \\ E_d &= (1-K) E_a \end{aligned}. \tag{8}$$

In order to calculate $s = s^{\text{init}} = s^{\text{final}}$, we use the reference frame of the propagating UHECR (a), denoted with $'$,

$$s = s^{\text{init}} = \left(E_a' + \epsilon'\right)^2 + \left(\epsilon'\right)^2 = s_a + 2\sqrt{s_a}\epsilon'. \tag{9}$$

Joining Equations (6)–(9) leads to

$$1 - K = \frac{s + s_d(K) - s_c(K)}{2s} + \cos\theta \sqrt{\left[\frac{s + s_d(K) - s_c(K)}{2s}\right]^2 - \frac{s_d(K)}{s}}, \tag{10}$$

where θ is the angle between the outgoing particles, c and d.

For the photodisintegration, the bound energy of the nucleus also needs to be taken into account. This can be achieved by shifting Equation (9) [66],

$$s = s_a + 2\sqrt{s_a}\epsilon' \to s = s_a + 2\sqrt{s_a}\left[\epsilon' - \left(\epsilon_{\text{thr}}^{\text{LI}}\right)'\right], \tag{11}$$

where $\left(\epsilon_{\text{thr}}^{\text{LI}}\right)'$ is the energy threshold in the NRF in a LI scenario.

Finally, the phase space of the interaction can be obtained as the combinations of E_a, ϵ', $\delta_{a,n}$, $\delta_{c,n}$ and $\delta_{d,n}$ for which Equation (10) has at least one real solution with $0 < K < 1$.

While LIV could be introduced independently for each particle species motivated by the underlying theory, kinematically and in a phenomenological approach for astroparticles [15], one can consider a MDR to hadronic particles ($\delta_{\text{had},n}$), such as protons (p), nuclei (A: the atomic mass), and pions (π), then, Equation (1) reads,

$$E_p^2 = p_p^2 + m_p^2 + \delta_{p,n} E_p^{n+2}\,, \tag{12}$$

$$E_A^2 = p_A^2 + m_A^2 + \delta_{A,n} E_A^{n+2}\,, \tag{13}$$

$$E_\pi^2 = p_\pi^2 + m_\pi^2 + \delta_{\pi,n} E_\pi^{n+2}\,. \tag{14}$$

Considering heavier nuclei as a superposition of A-protons,

$$\begin{aligned} E_A^2 &= p_A^2 + m_A^2 + \delta_{A,n} E_A^{n+2}\,, \implies \\ A^2 E_p^2 &= A^2 p_p^2 + A^2 m_p^2 + \delta_{A,n} A^{n+2} E_p^{n+2}, \end{aligned} \tag{15}$$

Then, using Equation (12) in Equation (15),

$$\delta_{p,n} = A^n \delta_{A,n}. \tag{16}$$

Following that LIV effects on pion production process relies on $\delta_{\pi,n} - \delta_{p,n}$ [15], and using the latest derivation in Equation (16), we consider,

$$\delta_{p,n} = A^n \delta_{A,n} = \delta_{\pi,n}/2 := \delta_{\text{had},n}. \quad (17)$$

Figures 7 and 8 show the energy threshold in the nucleus reference frame (NRF) for the pion production ($a \leftrightarrow p$, $c \leftrightarrow p$, $d \leftrightarrow \pi$) and for the photodisintegration ($a \leftrightarrow {}^{A}N$, $c \leftrightarrow {}^{A-1}N$, $d \leftrightarrow p$) for different positive LIV hadronic coefficients ($\delta_{\text{had},n}$). Similar to the case of UHE photons, the main effect of LIV is a pronounced increase in the energy threshold (and consequent decrease in the phase space), which becomes significant above given energy that depends on $\delta_{\text{had},n}$. Nevertheless, the effect is saturated for the highest energies differently from the pair production. This is because considered particles affected by LIV are present on both sides of the interaction. The effect of negative values of $\delta_{\text{had},n}$ is the opposite, decreasing the energy threshold. It is, however, suppressed by a decrease in the cross-section for lower background photon energies.

For the case of the photodisintegration, [66] presents a parameterization for the energy threshold in the NRF in the form of

$$\left(\epsilon_{\text{thr}}^{\text{LIV}}\right)' = \left(\epsilon_{\text{thr}}^{\text{LI}}\right)' + \frac{a(A, \delta_{\text{had},n}) \log(E_A/\text{eV})}{1 + \exp\{c(A, \delta_{\text{had},n})[\log(E_A/\text{eV}) - b(A, \delta_{\text{had},n})]\}}, \quad (18)$$

where a, b, and c have their own functional forms. UHECR propagation is usually solved via Monte Carlo simulations [43,67] and, thus, can be computationally costly. For that reason, parameterizing the calculation of LIV effects is a useful approach for speeding up the process.

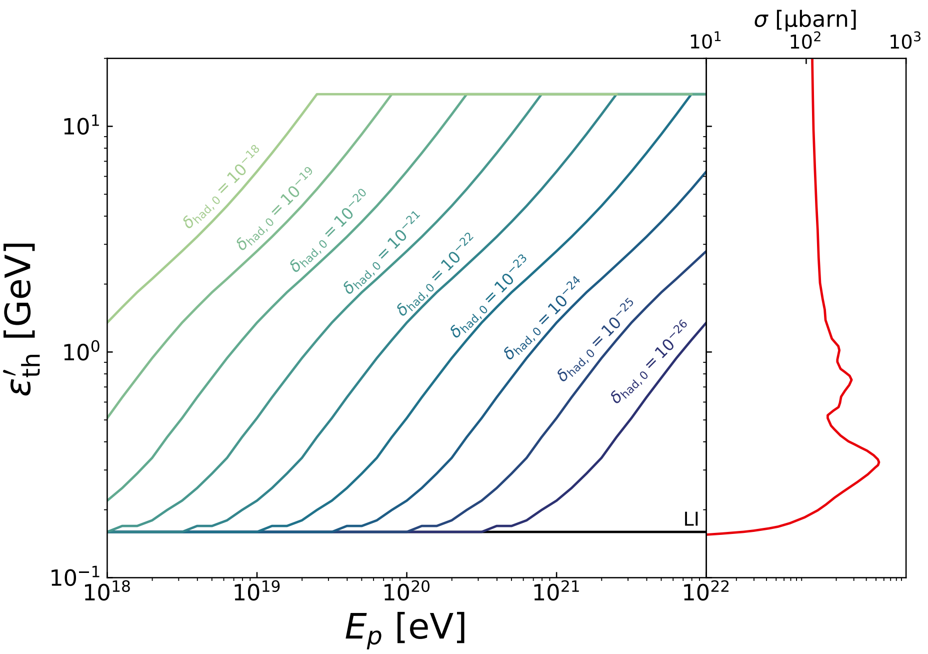

Figure 7. Energy threshold in the proton reference frame for the pion production. The black line shows the results for a LI assumption, while the different colored lines show the results for different LIV coefficients. The right panel shows the cross-section for that given energy, based on the parameterizations from [68].

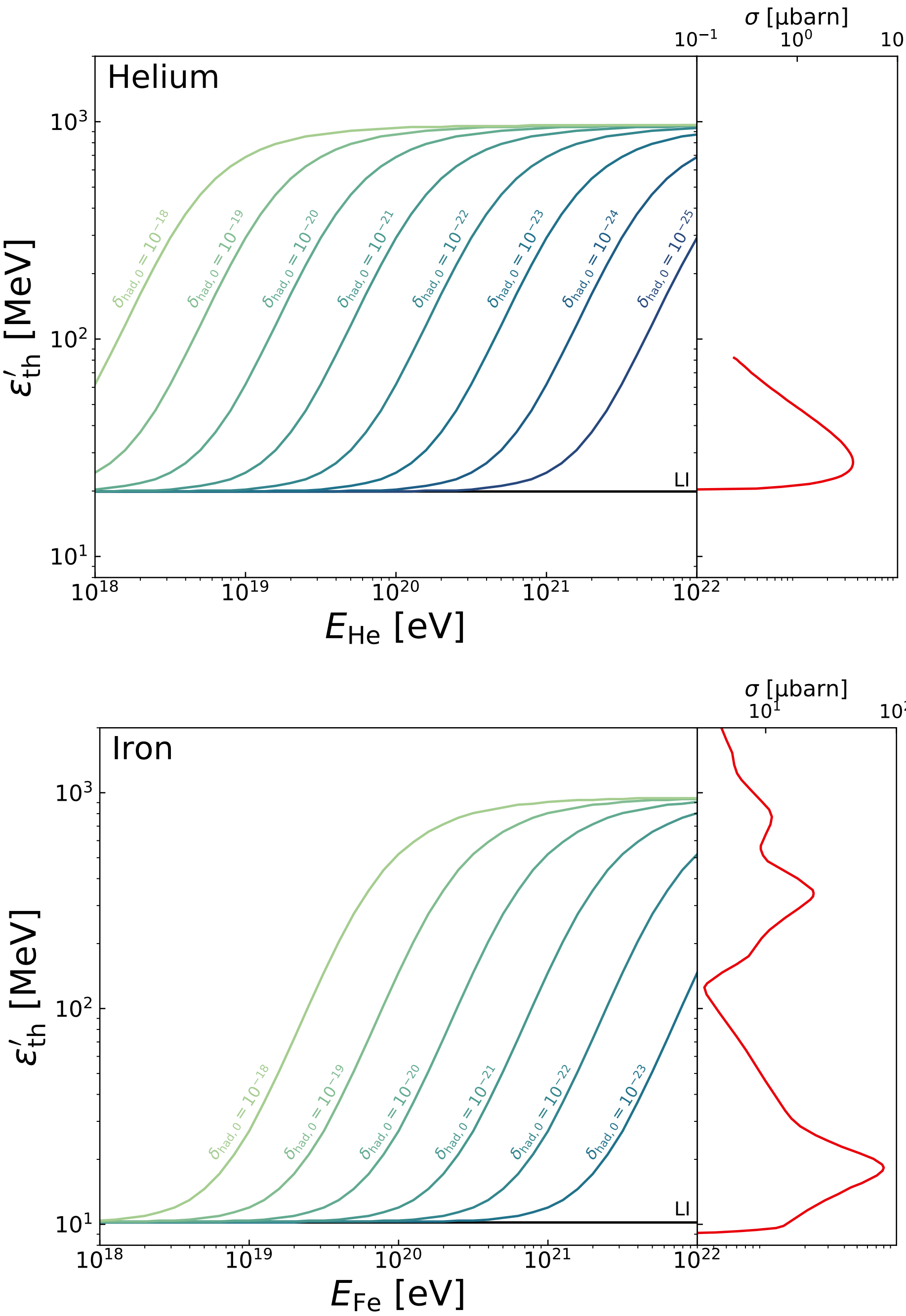

Figure 8. Energy threshold in the NRF for the photodisintegration. The black line shows the results for a LI assumption, while the different colored lines show the results for different LIV coefficients. The right panel shows the cross section for that given energy, based on the parameterizations from [69]. Top and bottom panels correspond to an initial nuclues of helium and iron, respectively.

4.2. Searching for LIV in UHECR Data

The pioneering work [70] on testing LIV with UHECR was motivated by the lack of the flux suppression at the highest energies as published by the Akeno Giant Air Shower Array (AGASA) [71]. The absence of a cut-off in the energy spectrum was interpreted as a hint of LIV in the highest energies which would cause the decrease in the interaction rate of UHECRs. However, the data measured by the High-Resolution Fly's Eye Cosmic Ray Detector (HiRes) [72] and by the Pierre Auger Observatory [73] have shown a suppression at the expected energy range. More recent results confirmed the suppression of the energy spectrum at 46 EeV with more than 5σ confidence level [45,46]. Accordingly, LIV studies [15,74,75] have changed their approach and focused on estimating the LIV scale for which the lack of suppression would be in contradiction with measurements and, thus, LIV limits could be imposed. These works considered a pure proton composition and found that the data at that time could be well described up to some small LIV coefficients, and limits ranging from $\delta_{p,0} \sim 10^{-22}$ were imposed.

The continuous operation of the Pierre Auger Observatory imposed another challenge to the LIV studies. The distributions of the depth in which the shower has its maximum energy deposit, $X_{\max}$, cannot be described by a pure proton composition and point towards an intermediate composition [47,48,76].

Over the last years, the Pierre Auger Collaboration has worked on searching for LIV imprints in their data [40,77,78] taking into account the measured energy spectrum and $X_{\max}$ distributions. A combined fit of both energy spectrum and $X_{\max}$ distributions was performed under different LIV assumptions. The effects of LIV on the photodisintegration were also considered to treat the chemical composition properly. The combined fit follows the procedure in [42], where a homogeneous distribution of UHECR sources emitting cosmic rays isotropically is considered, and the propagation is simulated with Monte Carlo methods.

The parameters of the energy spectrum used in the fit were shown to be sensitive to the LIV assumption. In particular, for intermediate to strong LIV coefficients, the spectral index shifts towards -2 as predicted in mechanisms based on Fermi acceleration [79–83]. The deviance of the fit decreases for LIV coefficients of the order $\delta_{\text{had},0} = 10^{-20 \text{ to } -21}$. Nevertheless, the absolute value of the deviance of the fit is quite large, with a reduced value of 300/101, indicating overall poor description of the data by the considered model. Therefore, even though the results point to a preference for models with fewer interactions during propagation, it was not possible to claim whether that could be caused by LIV or by other astrophysical features not covered in the simplistic model considered, such as a larger contribution of local sources, effects of structured extragalactic magnetic fields or differences in emission from different sources.

5. Conclusions and Future Prospects

In this review, we explore the potential of UHE astroparticles as probes for LIV, presenting the current status of phenomenological research in this area. In particular, we discuss LIV in two sectors, photonic and hadronic, using the latest data of UHE photons and UHECR, respectively.

For the case of UHE photons, we review a commonly used analytical approach for the shift in the energy threshold of the pair production due to LIV. This interaction drives the photon propagation, leading to an absorption of the initial flux that modulates the expected measurements on Earth. When LIV is considered, an increase in the energy threshold is predicted, resulting in fewer interactions and, thus, a higher expected flux on Earth. For some astrophysical and subluminal LIV scenarios, the predicted flux is stronger than current upper limits on the photon flux, and, consequently, limits on LIV can be imposed.

We discuss the model dependence of these results. We show that, within a range of reasonable astrophysical assumptions for the UHECR sources, the results can vary from complete insensitivity to LIV to the most restrictive LIV limits in the literature, $\delta_{\gamma,0} > -10^{-22}$, $\delta_{\gamma,1} > -10^{-42}\ \text{eV}^{-1} \left(E_{\text{LIV}}^{(1)} > 10^{42}\ \text{eV}\right)$ and $\delta_{\gamma,2} > -10^{-60}\ \text{eV}^{-2} \left(E_{\text{LIV}}^{(2)} > 10^{30}\ \text{eV}\right)$. We demonstrate that such a dependence is dominated by the maximum attainable energy at the sources, followed by the chemical composition. Low maximum power of acceleration of the sources contributes to insensitivity to LIV since most UHECR do not achieve enough energy to produce pions and, therefore, fewer UHE photons are emitted. Heavier compositions tend to lead to weaker LIV limits in the same direction, as the photodisintegration dominates over the pion production. In Figure 3, we present the LIV limits imposed by a collection of astrophysical models (Table 1). A comparison between the capabilities of each model to describe UHECR data is beyond the scope of this work, and, thus, neither of the limits (or absence of limits) are favored.

For the case of UHECR, we review the calculation of the effects of LIV in the kinematics of interactions which can be expressed in the form $a + b \to c + d$. In particular, we discuss the cases of the pion production and the photodisintegration, the leading energy losses for the highest energies. The inelasticity of the interaction can be reduced to a transcendental equation. For the photodisintegration, the energy threshold can be described by the parameterization proposed in [66], significantly speeding up the simulation of the UHECR propagation with LIV. Once more, the main LIV effect is an increase in the energy threshold, which leads to fewer interactions.

We briefly summarize the efforts of the community to describe the UHECR data considering LIV. Pioneer works have considered LIV in the proton sector and proposed to describe the energy spectrum measured by the AGASA, HiRes, and Pierre Auger Observatory experiments with a pure proton composition. Restrictive limits on the proton LIV coefficient were imposed. Nevertheless, a pure proton composition conflicts with current X_{max} measurements performed by the Pierre Auger Observatory. Recently, the Pierre Auger Collaboration has published a fit of the energy spectrum and X_{max} distributions under LIV assumptions. The results indicate a smaller deviance for a LIV scenario, however, a bad fit performance is seen overall and a more realistic model for the UHECR sources is needed for conclusive claims.

In summary, UHE astroparticles have proven to be a crucial tool in the search for a possible violation of Lorentz invariance. Current experiments provide precise and high statistics measurements, and a robust and widely spread framework was developed by many authors for the calculation of expected signatures of LIV in UHE data. Nevertheless, modeling UHECR is intricate due to their charged nature, the lack of knowledge about galactic and extragalactic magnetic fields, and the intrinsic fluctuations of extensive air-showers, which prevents an event-by-event composition measurement. Results on LIV strongly differ for different classes of models that can describe current UHE data. Planned upgrades of current experiments, such as AugerPrime [57,58] for the Pierre Auger Observatory and TAx4 [59] for the Telescope Array experiment, as well as future experiments such as the Probe of Extreme Multi-Messenger Astrophysics (POEMMA) [60] and Global Cosmic Ray Observatory (GCOS) [61] will be able to shrink the phase space of UHECR models, by constraining a possible proton component and better measuring the energy spectrum beyond the suppression. We are, thus, yet to see the full potential of UHE astroparticles as probes on LIV in the upcoming years.

Author Contributions: Conceptualization, R.G.L., H.M.-H. and V.d.S.; writing—original draft preparation, R.G.L.; writing—review and editing, H.M.-H. and V.d.S. All authors have read and agreed to the published version of the manuscript.

Funding: VdS acknowledges FAPESP support No. 2021/01089-1 and CNPq. VdS also acknowledges the National Laboratory for Scientific Computing (LNCC/MCTI, Brazil) for providing HPC resources of the SDumont supercomputer, which have contributed to the research results reported within this paper (http://sdumont.lncc.br, accessed on 8 June 2022).

Conflicts of Interest: The authors declare no conflict of interest. The funders had no role in the design of the study; in the collection, analyses, or interpretation of data; in the writing of the manuscript, or in the decision to publish the results.

Abbreviations

The following abbreviations are used in this manuscript:

AGASA	Akeno Giant Air Shower Array
CMB	Cosmic microwave background
CR	Cosmic rays
EBL	Extragalactic background bight
HiRes	High Resolution Fly's Eye Cosmic Ray Detector
LI	Lorentz invariant

LIV	Lorentz invariance violation
MDR	Modified dispersion relation
NRF	Nucleus reference frame
SM	Standard Model
UHE	Ultra-high energy
UHECR	Ultra-high-energy cosmic rays

References

1. Addazi, A.; Alvarez-Muniz, J.; Alves Batista, R.; Amelino-Camelia, G.; Antonelli, V.; Arzano, M.; Asorey, M.; Atteia, J.L.; Bahamonde, S.; Bajardi, F.; et al. Quantum gravity phenomenology at the dawn of the multi-messenger era—A review. *Prog. Part. Nucl. Phys.* **2022**, *125*, 103948. [CrossRef]
2. Alfaro, J. Quantum Gravity and Lorentz Invariance Violation in the Standard Model. *Phys. Rev. Lett.* **2005**, *94*, 221302. [CrossRef] [PubMed]
3. Amelino-Camelia, G. A phenomenological description of space-time noise in quantum gravity. *Nature* **2001**, *410*, 1065–1067. [CrossRef] [PubMed]
4. Bluhm, R. Observational Constraints on Local Lorentz Invariance. In *Springer Handbook of Spacetime*; Springer: Berlin, Germany, 2014; pp. 485–507. [CrossRef]
5. Colladay, D.; Kostelecky, V.A. Lorentz violating extension of the standard model. *Phys. Rev.* **1998**, *D58*, 116002. [CrossRef]
6. Ellis, J.; Mavromatos, N.E.; Nanopoulos, D.V. A Microscopic Recoil Model for Light-Cone Fluctuations in Quantum Gravity. *Phys. Rev. D* **1999**, *61*, 027503. [CrossRef]
7. Gambini, R.; Pullin, J. Nonstandard optics from quantum spacetime. *Phys. Rev.* **1999**, *59*, 124021.
8. Kostelecky, V.A.; Samuel, S. Spontaneous Breaking of Lorentz Symmetry in String Theory. *Phys. Rev.* **1989**, *D39*, 683. [CrossRef]
9. Nambu, Y. Quantum Electrodynamics in Nonlinear Gauge. *Suppl. Prog. Theor. Phys.* **1968**, *E68*, 190–195. [CrossRef]
10. Potting, R. Lorentz and CPT violation. *J. Phys. Conf. Ser.* **2013**, *447*, 012009. [CrossRef]
11. Martínez-Huerta, H.; Lang, R.G.; de Souza, V. Lorentz Invariance Violation Tests in Astroparticle Physics. *Symmetry* **2020**, *12*, 1232. [CrossRef]
12. Biteau, J.; Williams, D.A. The extragalactic background light, the Hubble constant, and anomalies: Conclusions from 20 years of TeV gamma-ray observations. *Astrophys. J.* **2015**, *812*, 60. [CrossRef]
13. Lang, R.G.; Martínez-Huerta, H.; de Souza, V. Improved limits on Lorentz invariance violation from astrophysical gamma-ray sources. *Phys. Rev. D* **2019**, *99*, 043015. [CrossRef]
14. Guedes Lang, R.; Martínez-Huerta, H.; de Souza, V. Limits on the Lorentz Invariance Violation from UHECR astrophysics. *Astrophys. J.* **2018**, *853*, 23. [CrossRef]
15. Scully, S.T.; Stecker, F.W. Lorentz Invariance Violation and the Observed Spectrum of Ultrahigh Energy Cosmic Rays. *Astropart. Phys.* **2009**, *31*, 220–225. [CrossRef]
16. Stecker, F.W.; Scully, S.T. Searching for New Physics with Ultrahigh Energy Cosmic Rays. *New J. Phys.* **2009**, *11*, 085003. [CrossRef]
17. Galaverni, M.; Sigl, G. Lorentz Violation in the Photon Sector and Ultra-High Energy Cosmic Rays. *Phys. Rev. Lett.* **2008**, *100*, 021102. [CrossRef]
18. Stecker, F.W.; Glashow, S.L. New tests of Lorentz invariance following from observations of the highest energy cosmic gamma-rays. *Astropart. Phys.* **2001**, *16*, 97–99. [CrossRef]
19. Stecker, F.W. Constraints on Lorentz invariance violating quantum gravity and large extra dimensions models using high energy gamma-ray observations. *Astropart. Phys.* **2003**, *20*, 85–90. [CrossRef]
20. Martínez-Huerta, H.; Pérez-Lorenzana, A. Restrictions from Lorentz invariance violation on cosmic ray propagation. *Phys. Rev.* **2017**, *D95*, 063001. [CrossRef]
21. Astapov, K.; Kirpichnikov, D.; Satunin, P. Photon splitting constraint on Lorentz Invariance Violation from Crab Nebula spectrum. *JCAP* **2019**, *1904*, 054. [CrossRef]
22. Schreck, M. Vacuum Cherenkov radiation for Lorentz-violating fermions. *Phys. Rev. D* **2017**, *96*, 095026. [CrossRef]
23. Schreck, M. (Gravitational) Vacuum Cherenkov Radiation. *Symmetry* **2018**, *10*, 424. [CrossRef]
24. Klinkhamer, F.R.; Schreck, M. New two-sided bound on the isotropic Lorentz-violating parameter of modified Maxwell theory. *Phys. Rev. D* **2008**, *78*, 085026. [CrossRef]
25. Amelino-Camelia, G.; Ellis, J.R.; Mavromatos, N.E.; Nanopoulos, D.V.; Sarkar, S. Tests of quantum gravity from observations of gamma-ray bursts. *Nature* **1998**, *393*, 763–765. [CrossRef]
26. Ellis, J.R.; Mavromatos, N.E.; Nanopoulos, D.V.; Sakharov, A.S. Quantum-gravity analysis of gamma-ray bursts using wavelets. *Astron. Astrophys.* **2003**, *402*, 409–424. [CrossRef]
27. Satunin, P. Two-sided constraints on Lorentz invariance violation from Tibet-ASγ and LHAASO very-high-energy photon observations. *Eur. Phys. J. C* **2021**, *81*, 750. [CrossRef]
28. Chen, L.; Xiong, Z.; Li, C.; Chen, S.; He, H. Strong constraints on Lorentz violation using new γ-ray observations around PeV. *Chin. Phys. C* **2021**, *45*, 105105. [CrossRef]
29. Kostelecky, V.A.; Russell, N. Data Tables for Lorentz and CPT Violation. *arXiv* **2008**, arXiv:hep-ph/0801.0287.

30. Aab, A. et al. [Pierre Auger Collaboration]. Search for photons with energies above 10^{18} eV using the hybrid detector of the Pierre Auger Observatory. *JCAP* **2017**, *04*, 009; Erratum in *JCAP* **2020**, *9*, E02. [CrossRef]
31. Rautenberg, J. et al. [Pierre Auger Collaboration]. Limits on ultra-high energy photons with the Pierre Auger Observatory. *PoS* **2019**, *ICRC2019*, 398.
32. Savina, P. [Pierre Auger Collaboration]. A search for ultra-high-energy photons at the Pierre Auger Observatory exploiting air-shower Universality. *PoS* **2021**, *ICRC2021*, 373.
33. Hooper, D.; Sarkar, S.; Taylor, A.M. The intergalactic propagation of ultrahigh energy cosmic ray nuclei. *Astropart. Phys.* **2007**, *27*, 199–212. [CrossRef]
34. Allard, D. Extragalactic propagation of ultrahigh energy cosmic-rays. *Astropart. Phys.* **2012**, *39–40*, 33–43. [CrossRef]
35. Galaverni, M.; Sigl, G. Lorentz Violation and Ultrahigh-Energy Photons. *Phys. Rev. D* **2008**, *78*, 063003. [CrossRef]
36. De Angelis, A.; Galanti, G.; Roncadelli, M. Transparency of the Universe to gamma rays. *Mon. Not. R. Astron. Soc.* **2013**. [CrossRef]
37. Breit, G.; Wheeler, J.A. Collision of Two Light Quanta. *Phys. Rev.* **1934**, *46*, 1087–1091. [CrossRef]
38. Gilmore, R.; Somerville, R.; Primack, J.; Dominguez, A. Semi-analytic modeling of the EBL and consequences for extragalactic gamma-ray spectra. *Mon. Not. Roy. Astron. Soc.* **2012**, *422*, 3189. [CrossRef]
39. Gervasi, M.; Tartari, A.; Zannoni, M.; Boella, G.; Sironi, G. The Contribution of the Unresolved Extragalactic Radio Sources to the Brightness Temperature of the Sky. *Astrophys. J.* **2008**, *682*, 223–230. [CrossRef]
40. Abreu, P.; Aglietta, M.; Albury, J.; Allekotte, I.; Cheminant, K.A.; Almela, A.; Alvarez-Muñiz, J.; Batista, R.A.; Anastasi, G.; Anchordoqui, L.; et al. Testing effects of Lorentz invariance violation in the propagation of astroparticles with the Pierre Auger Observatory. *J. Cosmol. Astropart. Phys.* **2022**, *2022*, 023. [CrossRef]
41. Kampert, K.H.; Sarkar, B. Ultra-High Energy Photon and Neutrino Fluxes in Realistic Astrophysical Scenarios. In Proceedings of the International Cosmic Ray Conference, Beijing, China, 11–18 August 2011; Volume 2, p. 198. [CrossRef]
42. Aab, A. et al. [Pierre Auger Collaboration]. Combined fit of spectrum and composition data as measured by the Pierre Auger Observatory. *JCAP* **2017**, *04*, 038; Erratum in *JCAP* **2018**, *03*, E02. [CrossRef]
43. Batista, R.; Dundovic, A.; Erdmann, M.; Kampert, K.H.; Kuempel, D.; Müller, G.; Sigl, G.; van Vliet, A.; Walz, D.; Winchen, T. CRPropa 3—A Public Astrophysical Simulation Framework for Propagating Extraterrestrial Ultra-High Energy Particles. *JCAP* **2016**, *05*, 038. [CrossRef]
44. Settimo, M.; De Domenico, M.; Lyberis, H. EleCa: A Monte Carlo code for the propagation of extragalactic photons at ultra-high energy. *Nucl. Phys. B Proc. Suppl.* **2013**, *239–240*, 279–282. [CrossRef]
45. Aab, A. et al. [Pierre Auger Collaboration]. Measurement of the cosmic-ray energy spectrum above 2.5×10^{18} eV using the Pierre Auger Observatory. *Phys. Rev. D* **2020**, *102*, 062005. [CrossRef]
46. Aab, A. et al. [Pierre Auger Collaboration]. Features of the Energy Spectrum of Cosmic Rays above 2.5×10^{18} eV using the Pierre Auger Observatory. *Phys. Rev. Lett.* **2020**, *125*, 121106. [CrossRef]
47. Aab, A. et al. [Pierre Auger Collaboration]. Depth of maximum of air-shower profiles at the Pierre Auger Observatory. II. Composition implications. *Phys. Rev. D* **2014**, *90*, 122006. [CrossRef]
48. Aab, A. et al. [Pierre Auger Collaboration]. Depth of Maximum of Air-Shower Profiles at the Pierre Auger Observatory: Measurements at Energies above $10^{17.8}$ eV. *Phys. Rev. D* **2014**, *90*, 122005. [CrossRef]
49. Abbasi, R. et al. [Pierre Auger Collaboration]. Joint analysis of the energy spectrum of ultra-high-energy cosmic rays as measured at the Pierre Auger Observatory and the Telescope Array. *PoS* **2021**, *ICRC2021*, 337. [CrossRef]
50. Berezinsky, V.; Gazizov, A.Z.; Grigorieva, S.I. On astrophysical solution to ultrahigh-energy cosmic rays. *Phys. Rev. D* **2006**, *74*, 043005. [CrossRef]
51. Allard, D.; Busca, N.G.; Decerprit, G.; Olinto, A.V.; Parizot, E. Implications of the cosmic ray spectrum for the mass composition at the highest energies. *JCAP* **2008**, *10*, 033. [CrossRef]
52. Aloisio, R.; Berezinsky, V.; Blasi, P. Ultra high energy cosmic rays: Implications of Auger data for source spectra and chemical composition. *JCAP* **2014**, *10*, 020. [CrossRef]
53. Taylor, A.M.; Ahlers, M.; Hooper, D. Indications of Negative Evolution for the Sources of the Highest Energy Cosmic Rays. *Phys. Rev. D* **2015**, *92*, 063011. [CrossRef]
54. Unger, M.; Farrar, G.R.; Anchordoqui, L.A. Origin of the ankle in the ultrahigh energy cosmic ray spectrum, and of the extragalactic protons below it. *Phys. Rev. D* **2015**, *92*, 123001. [CrossRef]
55. Muzio, M.S.; Unger, M.; Farrar, G.R. Progress towards characterizing ultrahigh energy cosmic ray sources. *Phys. Rev. D* **2019**, *100*, 103008. [CrossRef]
56. Luce, Q.; Marafico, S.; Biteau, J.; Condorelli, A.; Deligny, O. Observational constraints on cosmic-ray escape from UHE accelerators. *arXiv* **2022**, arXiv:astro-ph.HE/2207.08092.
57. Martello, D. et al. [Pierre Auger Collaboration]. The Pierre Auger Observatory Upgrade. *PoS* **2017**, *ICRC2017*, 383.
58. Cataldi, G. et al. [Pierre Auger Collaboration]. The upgrade of the Pierre Auger Observatory with the Scintillator Surface Detector. *PoS* **2021**, *ICRC2021*, 251.
59. Abbasi, R.U. et al. [Pierre Auger Collaboration]. Surface detectors of the TAx4 experiment. *Nucl. Instrum. Meth. A* **2021**, *1019*, 165726. [CrossRef]

60. Olinto, A.V. et al. [Pierre Auger Collaboration]. The POEMMA (Probe of Extreme Multi-Messenger Astrophysics) observatory. *JCAP* **2021**, *06*, 007. [CrossRef]
61. Hörandel, J.R. GCOS-The Global Cosmic Ray Observatory. *PoS* **2021**, *ICRC2021*, 027. [CrossRef]
62. Greisen, K. End to the cosmic ray spectrum? *Phys. Rev. Lett.* **1966**, *16*, 748–750. [CrossRef]
63. Zatsepin, G.; Kuzmin, V. Upper limit of the spectrum of cosmic rays. *JETP Lett.* **1966**, *4*, 78–80.
64. Taylor, A.M.; Ahlers, M.; Aharonian, F.A. The need for a local source of UHE CR nuclei. *Phys. Rev. D* **2011**, *84*, 105007. [CrossRef]
65. Lang, R.G.; Taylor, A.M.; Ahlers, M.; de Souza, V. Revisiting the distance to the nearest ultrahigh energy cosmic ray source: Effects of extragalactic magnetic fields. *Phys. Rev. D* **2020**, *102*, 063012. [CrossRef]
66. Lang, R.G. Effects of Lorentz Invariance Violation on the Ultra-High Energy Cosmic Rays Spectrum. Master's Thesis, University of São Paulo, São Paulo, Brazil, 2017. [CrossRef]
67. Aloisio, R.; Boncioli, D.; Di Matteo, A.; Grillo, A.F.; Petrera, S.; Salamida, F. SimProp v2r4: Monte Carlo simulation code for UHECR propagation. *JCAP* **2017**, *11*, 009. [CrossRef]
68. Mucke, A.; Engel, R.; Rachen, J.P.; Protheroe, R.J.; Stanev, T. SOPHIA: Monte Carlo simulations of photohadronic processes in astrophysics. *Comput. Phys. Commun.* **2000**, *124*, 290–314. [CrossRef]
69. Rachen, J.P. Interaction Processes and Statistical Properties of the Propagation of Cosmic Rays in Photon Backgrounds. Ph.D. Thesis, Max-Planck-Institute for Radioastronomy, Bonn, Germany, 1996.
70. Stecker, F.W.; Scully, S.T. Lorentz invariance violation and the spectrum and source power of ultrahigh energy cosmic rays. *Astropart. Phys.* **2005**, *23*, 203–209. [CrossRef]
71. Takeda, M.; Sakaki, N.; Honda, K.; Chikawa, M.; Fukushima, M.; Hayashida, N.; Inoue, N.; Kadota, K.; Kakimoto, F.; Kamata, K.; et al. Energy determination in the Akeno Giant Air Shower Array experiment. *Astropart. Phys.* **2003**, *19*, 447–462. [CrossRef]
72. Abbasi, R.U.; Abu-Zayyad, T.; Allen, M.; Amman, J.F.; Archbold, G.; Belov, K.; Belz, J.W.; Zvi, S.B.; Bergman, D.R.; Blake, S.A.; et al. First observation of the Greisen-Zatsepin-Kuzmin suppression. *Phys. Rev. Lett.* **2008**, *100*, 101101. [CrossRef] [PubMed]
73. Abraham, J.; Abreu, P.; Aglietta, M.; Aguirre, C.; Allard, D.; Allekotte, I.; Allen, J.; Allison, P.; Alvarez-Muniz, J.; Ambrosio, M.; et al. Observation of the suppression of the flux of cosmic rays above 4×10^{19}eV. *Phys. Rev. Lett.* **2008**, *101*, 061101. [CrossRef] [PubMed]
74. Bi, X.J.; Cao, Z.; Li, Y.; Yuan, Q. Testing Lorentz Invariance with Ultra High Energy Cosmic Ray Spectrum. *Phys. Rev. D* **2009**, *79*, 083015. [CrossRef]
75. Maccione, L.; Taylor, A.M.; Mattingly, D.M.; Liberati, S. Planck-scale Lorentz violation constrained by Ultra-High-Energy Cosmic Rays. *JCAP* **2009**, *04*, 022. [CrossRef]
76. de Souza, V. Testing the agreement between the $X_{\max}$ distributions measured by the Pierre Auger and Telescope Array Observatories. *PoS* **2018**, *ICRC2017*, 522. [CrossRef]
77. Boncioli, D. et al. [Pierre Auger Collaboration]. Probing Lorentz symmetry with the Pierre Auger Observatory. *PoS* **2018**, *ICRC2017*, 561. [CrossRef]
78. Lang, R.G. et al. [Pierre Auger Collaboration]. Testing Lorentz Invariance Violation at the Pierre Auger Observatory. *PoS* **2019**, *ICRC2019*, 450. [CrossRef]
79. Fermi, E. On the origin of the Cosmic Radiation. *Phys. Rev.* **1949**, *75*, 1169–1174. [CrossRef]
80. Axford, W. Acceleration of Cosmic Rays by Shock Waves. *Ann. N. Y. Acad. Sci.* **2006**, *375*, 297–313. [CrossRef]
81. Krymskii, G.F. A regular mechanism for the acceleration of charged particles on the front of a shock wave. *Akad. Nauk SSSR Dokl.* **1977**, *234*, 1306–1308. Available online: https://ui.adsabs.harvard.edu/abs/1977DoSSR.234.1306K (accessed on 8 December 2020).
82. Bell, A.R. The acceleration of cosmic rays in shock fronts. I. *Mon. Not. R. Astron. Soc.* **1978**, *182*, 147–156. [CrossRef]
83. Blandford, R.; Ostriker, J. Particle Acceleration by Astrophysical Shocks. *Astrophys. J. Lett.* **1978**, *221*, L29–L32. [CrossRef]